Cabbeling and the density of the North Pacific Intermediate Water quantified by an inverse method

Jae-Yul Yun
Research Institute of Oceanography, Seoul National University, Seoul, South Korea

Lynne D. Talley
Scripps Institution of Oceanography, University of California, San Diego, La Jolla, California, USA

Received 20 May 2002; revised 2 December 2002; accepted 14 February 2003; published 15 April 2003.

[1] North Pacific Intermediate Water (NPIW), defined as the main salinity minimum in the subtropical North Pacific, at a density of 26.7–26.8σ_θ, is denser than the winter surface water in the Oyashio which is the source of the salinity minimum. We showed previously that cabbeling and double diffusion during mixing between the Oyashio water and more saline Kuroshio water can account for the density increase from the surface source water to the salinity minimum. An inverse method is employed herein to quantify the effect of cabbeling, using CTD data from the western North Pacific. The difference between proportional mixing between parcels of Oyashio and Kuroshio waters and mixing along isopycnals is exploited to compute the convergence of water into density layers. The diapycnal transport convergence associated with cabbeling into the NPIW density layer is estimated to be 0.56 Sv for an assumed turnover time of 1 year in the region between 142°E and 152°E. Diapycnal transport convergences in the regions 152°E–165°E, 165°E–175°W, and 175°W–136°W are similarly estimated by assuming longer turnover times. We estimate that the total diapycnal transport convergence into the NPIW density layer may be up to 2.3 Sv in the entire NPIW region. *INDEX TERMS:* 4283 Oceanography: General: Water masses; 4568 Oceanography: Physical: Turbulence, diffusion, and mixing processes; 4279 Oceanography: General: Upwelling and convergences; *KEYWORDS:* NPIW, cabbeling, inverse method, diapycnal transport, diapycnal volume convergence

Citation: Yun, J.-Y., and L. D. Talley, Cabbeling and the density of the North Pacific Intermediate Water quantified by an inverse method, *J. Geophys. Res.*, *108*(C4), 3118, doi:10.1029/2002JC001482, 2003.

1. Introduction

[2] The source and formation process for the North Pacific Intermediate Water (NPIW), which is chiefly characterized by a salinity minimum at 26.7 to 26.8σ_θ, have been a focus of interest for many years. Following a series of earlier studies [e.g., *Sverdrup et al.*, 1942; *Reid*, 1965, 1973; *Kawai*, 1972; *Hasunuma*, 1978; *Talley*, 1985, 1988, 1991; *Van Scoy et al.*, 1991] on various aspects of the NPIW, *Talley* [1993] presented a comprehensive study of the distribution and formation of the NPIW. *Talley et al.* [1995] and *Yasuda et al.* [1996] focused on the creation of the salinity minimum in the Mixed Water Region (MWR), which lies between the separated Kuroshio and Oyashio just east of Japan. In these latter studies it was concluded that the salinity minimum results from frontal subsidence of relatively fresh subpolar surface water beneath warmer, saltier subtropical water.

[3] In work by *Talley et al.* [1995] and *Talley* [1997] it was shown that the new NPIW flowing eastward within the MWR is a mixture of waters of Kuroshio and Oyashio origin, in percentages of about 55% and 45%, respectively. Thus mixing appears to occur rapidly within the MWR. The mixing may include turbulent and double diffusive processes. In all mixing of waters of differing temperature and salinity, cabbeling [*Witte*, 1902; *Stommel*, 1960; *Foster*, 1972; *McDougall*, 1984] is inevitable because of the nonlinear equation of state. Cabbeling is strongest when differences in temperatures and salinities between the source water masses are large. A much less important effect is the greater nonlinearity in density at lower temperature and higher salinity, which weakly strengthens the cabbeling effect. *You et al.* [2000] found from their analyses of the World Ocean Circulation Experiment sections and historical hydrography that the double diffusion is a major cause of NPIW formation and transformation in the Gulf of Alaska and in the northwestern subpolar gyre and the Okhotsk Sea. *Talley and Yun* [2001] showed that cabbeling and possibly double diffusion during mixing of the subtropical and subpolar waters in the MWR are responsible for the higher density of the NPIW salinity minimum compared with the density of the Oyashio winter surface water that provides the freshness for the salinity minimum. Cabbeling is a source of error in the 55/45% estimates of the Kuroshio and Oyashio contributions given by *Talley* [1997].

[4] The purpose of this paper is to better quantify the mixing of subtropical and subpolar source waters in pro-

0148-0227/03/2002JC001482$09.00

ducing the NPIW, to show the extent to which cabbeling increases the NPIW density to $26.7-26.8\sigma_\theta$ (values greater than the density of the Oyashio winter surface water which is the fresh water source), and to quantify the transport into the NPIW density layer from lighter densities that results from cabbeling. In order to demonstrate this process we use an inverse method that best describes the observed CTD data in a least squares sense as a mixture of fractional contributions from the subtropical and the subpolar water masses. In this study we do not consider the possible role of double diffusion, which can also increase the density of the intrusive salinity minima, and whose potential role was discussed by *You et al.* [2000], *Talley and Yun* [2001] and *You* [2003]. *You* [2003] used formal expressions from *McDougall and You* [1990] for cabbeling, thermobaricity and double diffusion to estimate the diapycnal transports in the NPIW density range for the whole of the North Pacific. He found that the transports are largest in the Mixed Water Region, due to the largest horizontal gradients of temperature and salinity on isopycnals there, which is also the basis for the cabbeling study of *Talley and Yun* [2001] using data from the MWR. The transport quantified here is based on an entirely independent method, looking at the cabbeling impact on each water parcel in the data sets considered, with specific source waters for the mixture.

[5] In sections 2 and 3 the method and the data are described. The water mass distributions along meridional sections and on isopycnal surfaces are discussed in section 4. In section 5 the cabbeling process as a mechanism that sets the density of the NPIW is discussed and mass convergence into the NPIW density layer is computed.

2. Method

[6] Mixing ratios have been used for decades to quantify the relative amounts of various source waters in a given water mass. Practitioners have usually assumed constituents of uniform properties (point sources) at different densities. *Mackas et al.* [1987] applied a least squares (inverse) method to traditional water mass analysis, using concentrations of six tracers to find the mixture of five source water types that best described in a weighted least squares sense the composition of a particular water sample. *Maamaatuaiahutapu et al.* [1992] applied the Mackas method to the water mass composition in the Brazil-Malvinas confluence region, also using six tracers. Multiple tracers are rarely available and, in some regions, the water mass composition is so simple that temperature and salinity alone can be used to estimate the fractional contributions. The assumption of point sources of waters made in previous analyses is weak since the source waters that mix often have a large density and depth range.

[7] In the western North Pacific, in the MWR, the water mass composition is relatively simple, with two major water masses occupying a large density range. These waters, of Kuroshio and Oyashio origin, differ significantly from each other over a depth range of more than 1000 m, and a density range from the surface density to about $27.6\sigma_\theta$ [*Talley*, 1993; *Talley et al.*, 1995]. They contrast strongly in temperature/salinity and also in oxygen content. A third water mass, the Tsugaru Water, mainly affects densities lower than those considered here [*Talley*, 1993]. From these water "masses" comes a mixture that ventilates the deeper part of the upper subtropical gyre (500 to 1000 m). This mixture can be termed the NPIW in its total density range; the top of the mixture is the salinity minimum, which is also identified more narrowly as the NPIW.

[8] The MWR is the best sampled region in the world in terms of temperature and salinity. There are also many years of oxygen observations. Other tracer measurements have not been made routinely there. The strong contrast in subtropical and subpolar waters in just temperature and salinity makes it possible to quantify the relative amounts using only temperature and salinity [*Talley et al.*, 1995; *Talley and Yun*, 2001]. We apply the *Mackas et al.* [1987] least squares method to this region, extending it by assuming isopycnal mixing of the two source waters, which are clearly differentiated over a large density range. CTD data are used in order to take advantage of high vertical resolution. The Mackas et al. method was chosen because we initially intended to take advantage of the oxygen data set. However the water masses are so well differentiated in temperature and salinity that oxygen was not required. The least squares method on the other hand has lent itself well here to quantification of the misfit between assumed isopycnal mixing and the actual proportional mixing along straight lines in temperature/salinity (i.e., cabbeling), allowing us to compute convergence and divergence in isopycnal layers.

[9] It is assumed that heat, salt, and mass are conserved. Thus the analysis is applied only to densities higher than that of the Oyashio winter surface layer. The total heat, salt content, and mass of a water parcel are $c_p\rho VT$, ρVS, and ρV, respectively, where ρ is potential density, V volume, T potential temperature, S salinity and c_p the specific heat at constant pressure. Although c_p is a function of T and S, we assume that it is constant because the effect of its variation is negligible [*Fofonoff*, 1956]. Heat, salt and mass conservation in the case of mixing two water parcels can be written as

$$\begin{aligned} \rho_1 V_1 T_1 + \rho_2 V_2 T_2 &= \rho VT, \\ \rho_1 V_1 S_1 + \rho_2 V_2 S_2 &= \rho VS, \\ \rho_1 V_1 + \rho_2 V_2 &= \rho V, \end{aligned} \tag{1}$$

where the subscripts 1 and 2 indicate the subtropical and the subpolar water masses, respectively, and the variables without subscripts are the observations. Thus our problem is fitting the data to a model of two source water masses, which is an inverse method. As in work by *Talley* [1997] and *Talley and Yun* [2001], it is assumed that mixing occurs primarily along isopycnals, $\rho_1 = \rho_2 = \rho_0$. We make this assumption, which differs from that of *Mackas et al.* [1987] and others, because the actual mixing process in the local region of our study must occur between water parcels that are adjacent, and which therefore must have almost the same initial density. The mixing most likely occurs at vertical interfaces between interleaving layers of the two water masses, as described by *Joyce* [1977]; the densities of the interleaving layers are almost the same, as observed in actual interleaving in the MWR [*Talley and Yun*, 2001].

[10] Initially, a linear equation of state is assumed; cabbeling is thus not included. The extent to which the nonlinear equation of state and hence cabbeling change the final density of the mixture are considered in section 5, where they are the basis for estimating a diapycnal transport rate. Defining $x_1 = \rho_0 V_1/\rho V$ and $x_2 = \rho_0 V_2/\rho V$, so that x_1 and x_2 are the fractional contributions of the source water masses, equation (1) is written as

$$x_1 T_1 + x_2 T_2 = T,$$
$$x_1 S_1 + x_2 S_2 = S, \tag{2}$$
$$x_1 + x_2 = 1.$$

Talley [1997] and *Talley and Yun* [2001] used either temperature or salinity alone and an assumption of isopycnal mixing to compute the relative fractions of Kuroshio and Oyasio waters. The approach (equation (1)) here also explicitly assumes isopycnal mixing, although we know that the mixture must be denser due to cabbeling. Equation (1) will yield an improvement to our previous estimates because the curvature of the isopycnals in potential temperature/salinity means that fractions computed using either temperature or salinity alone differ from each other, with the difference depending on the distance of a straight line in potential temperature/salinity space from the curved isopycnals, hence depending on the amount of cabbeling. This is illustrated in Figure 1. The method we use here weights temperature and salinity equally, which is an improvement. Moreover, the error in determining the relative fraction of the two water masses is due to the separation between the straight line (mixing) and the curved isopycnal for a given water parcel, since otherwise the solutions for x_1 and x_2 are exactly determined.

[11] Equation (2) can be written in matrix form as

$$\mathbf{Ax} = \mathbf{b}, \tag{3}$$

$$\text{where } \mathbf{A} = \begin{bmatrix} T_1 T_2 \\ S_1 S_2 \\ 11 \end{bmatrix}, \ \mathbf{x} = \begin{bmatrix} x_1 \\ x_2 \end{bmatrix} \text{ and } \mathbf{b} = \begin{bmatrix} T \\ S \\ 1 \end{bmatrix}$$

Equation (3) is the same form as used by *Mackas et al.* [1987] except for the number of tracers. **A** is a source definition matrix and its column vectors are tracer properties for its corresponding source water mass, **b** is the data vector and assumed to be a mixture of the source water masses described by **A**, and **x** is then the set of solutions giving the best fitting fractional contribution of each water mass.

[12] Only approximate equality between **Ax** and **b** is assumed in equation (3) because of errors in the data and in the model assumptions (particularly of linear mixing of two sources). The solution for the vector **x** minimizes the weighted sum of squares of differences between the measured and estimated tracer concentration,

$$\mathrm{E} = (\mathbf{Ax} - \mathbf{b})^{\mathrm{T}} \mathbf{W}^{-1} (\mathbf{Ax} - \mathbf{b}). \tag{4}$$

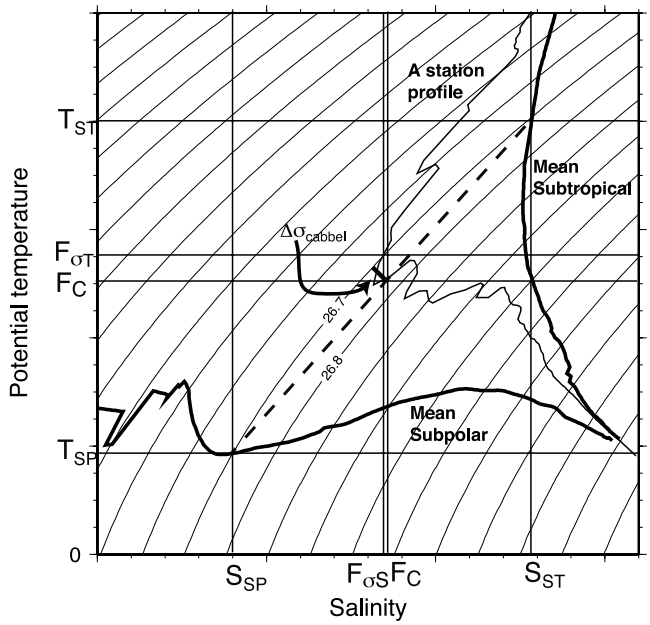

Figure 1. Schematic of the mixing and diapycnal transport concepts. T_{ST}, S_{ST} and T_{SP}, S_{SP} are the potential temperature and salinity of subtropical and subpolar source waters for a sample isopycnal. T_σ, S_σ and T_C, S_C are the potential temperature and salinity on a sample mixture profile, at the source water density and along the straight line connecting the source waters, respectively. $F_{\sigma S}$ is the fraction of subpolar water in the mixture if calculated along the isopycnal and using salinity for the relative proportion. $F_{\sigma T}$ is the fraction of the same if using potential temperature for the relative proportion. F_C is the fraction of subpolar water in the mixture if using T_C, S_C as the properties of the mixture. Because of the curvature of isopycnals in the T, S plane, $F_{\sigma S} < F_C < F_{\sigma T}$. F_C is the correct fraction if cabbeling is the only diapycnal process. $\Delta\sigma_{cabbel}$ is the increase in density due to cabbeling.

The weighting is provided by the inverse of **W**, the dispersion matrix of the error vector **Ax** − **b**. For simplicity and because of the unknown nature of variability in each element of **A** and **b**, we only take into account the measurement uncertainty associated with the observations, as in the work by *Mackas et al.* [1987].

[13] If **W** is symmetric and non-negative, it has the singular value decomposition $\mathbf{W} = \mathbf{U}\Lambda\mathbf{U}^{\mathrm{T}}$, where the diagonal elements of Λ are nonnegative and thus $\mathbf{W}^{-1} = (\mathbf{U}^{\mathrm{T}})^{-1}\Lambda^{-1}\mathbf{U}^{-1}$. From orthogonality of **U**, $\mathbf{W}^{-1} = \mathbf{U}\Lambda^{-1}\mathbf{U}^{\mathrm{T}}$, since $(\mathbf{U}^{\mathrm{T}})^{-1} = \mathbf{U}$. Therefore, equation (4) becomes

$$\mathrm{E} = (\mathbf{Gx} - \mathbf{d})^{\mathrm{T}} (\mathbf{Gx} - \mathbf{d}), \tag{5}$$

where $\mathbf{G} = \Lambda^{-1/2}\mathbf{U}^{\mathrm{T}}\mathbf{A}$ and $\mathbf{d} = \Lambda^{-1/2}\mathbf{U}^{\mathrm{T}}\mathbf{b}$.

[14] Since there are three equations and two unknowns, this is an overdetermined problem. The solution technique for **x** is described by *Menke* [1989] and *Mackas et al.* [1987]. The sensitivity of the solutions to the dispersion matrix **W** was checked and it was found that the solutions are stable for reasonable choices of the measurement error for *T* and *S*. A conservative estimate of CTD measurement error of 0.005 is used for both temperature and salinity.

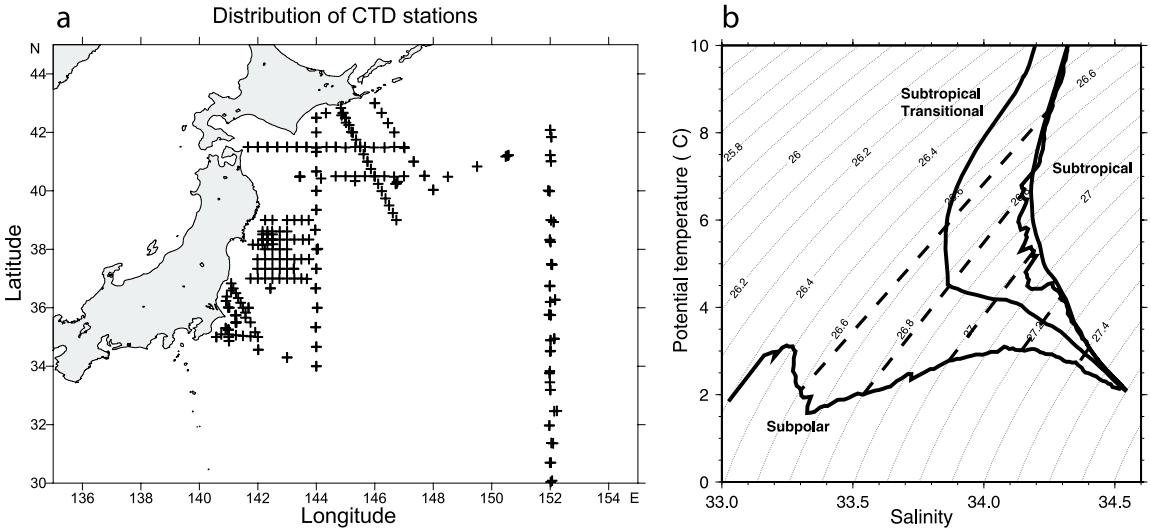

Figure 2. (a) Distribution of CTD stations. (b) Potential temperature versus salinity for the average subtropical and subpolar source waters. The smoother subtropical curve and the subpolar curve are from *Talley and Yun* [2001], and the less smooth subtropical curve is the one computed here. These are similar to those of *Talley et al.* [1995] and *Yasuda et al.* [1996]. Also shown are contours of potential density referenced to 0 dbar. Mixing of the source waters should occur along the indicated straight lines, resulting in cabbeling or an increase in density of the mixture. Cabbeling is largest where the source waters differ the most. The greatest density increases, of about 0.09 and $0.07\sigma_\theta$, are at $26.4\sigma_\theta$ and $26.6\sigma_\theta$, respectively.

[15] Following *Mackas et al.* [1987], a nonnegativity constraint is applied to the fractional contributions x_1 and x_2. The implication of this constraint is simple. When temperature and salinity are greater than those of the subtropical source water or lower than those of the subpolar source, a positive solution is forced in a least squares sense. The best fit error is larger than in the case when T and S fall within the ranges of the two source water masses (see Figure 4 below). The goodness of fit is measured by the root mean square of E in equation (5).

3. Data

[16] In order to estimate the fractional contributions of the subtropical and the subpolar source waters along isopycnal surfaces, CTD data collected in 1989 (April–June), 1981 (May), and 1982 (May–June) in the western North Pacific were analyzed (Figure 2a and Table 1). The area covered by these data sets is 33.8°N–42.8°N, 140.5°E–152.2°E. *Talley et al.* [1995] presented the property distributions along the sections and discussed the formation of NPIW in this region. *Niiler et al.* [1985] collected the 1981 and 1982 data and discussed the properties thoroughly. *Talley and Yun* [2001] used these data to show the impact of cabbeling and double diffusion in creation of the subtropical form of NPIW from the mixture of Oyashio and Kuroshio source waters. The CTD sections at 165°E and 175°W, which were observed in 1983 and 1984 and discussed by *Joyce* [1987], are also used in this analysis (Table 1).

[17] Potential temperature and salinity were interpolated to $0.01\sigma_\theta$ intervals between $26.4\sigma_\theta$ and $27.6\sigma_\theta$. Lower densities are found in the Oyashio water only seasonally; we specifically chose to apply the analysis only at densities that are not strongly affected by surface fluxes. *Talley* [1991] showed that the influence of Okhotsk Sea ventilation extends through diapycnal mixing to about $27.6\sigma_\theta$, which is the density at the bottom of the deepest sill connecting the Okhotsk Sea and the Pacific. This is also about the highest density of clear differences between subtropical and subpolar waters, probably as a result of Okhotsk Sea processes.

4. Water Mass Distribution in the Western North Pacific

[18] In this section we present the fractional contributions of Kuroshio (subtropical) and Oyashio (subpolar) waters to the mixtures in the MWR. Our results are an improvement over those based purely on proportional mixing, as in the

Table 1. CTD Data Used for Analysis

Section	Ship	Dates	No. of Stations	Latitude, °N	Station Number	Reference
144°E	Kofu-maru	05/05/89–05/08/89	14	34.00–42.50	41–45	*Talley et al.* [1995]
152°E	T. Washington	05/13/81–05/28/81	20	27.73–40.10	3–22	*Niiler et al.* [1985]
152°E	T. Thompson	05/25/82–06/05/82	25	27.73–42.08	3–27	*Niiler et al.* [1985]
165°E	T. Thompson	11/25/83–12/04/83	19	30.50–43.00	10–28	*Joyce* [1987]
165°E	T. Thompson	09/27/84–10/08/84	27	29.00–44.00	3–29	*Joyce* [1987]
175°W	T. Thompson	10/12/84–10/28/84	28	24.66–44.00	1–2, 30–55	*Joyce* [1987]

work by *Talley* [1997] and *Talley and Yun* [2001], since they provide the best fit for both temperature and salinity mixing. The ambiguity of the previous approach is apparent in Figure 1 and in *Talley*'s [1997]Figure 2b, in which the fraction of subtropical water in the subtropical transitional water (new NPIW) in the MWR is calculated from temperature and salinity separately (e.g., $F_{\sigma S}$ and $F_{\sigma T}$ in Figure 1). The least squares method provides essentially the mean between these two estimates (F_C in Figure 1). Simple proportional mixing provides a reasonable qualitative picture of the relative contributions, as in the work by *Talley and Yun* [2001]. *Zhang and Hanawa* [1993] looked at the proportions of subpolar and subtropical waters (defined near the western boundary) across the subarctic North Pacific, using synoptic meridional sections in the western Pacific and the averaged data from *Levitus* [1982] for the whole region, and obtained results qualitatively like those presented here. The least squares technique is most useful in section 5 below where the misfit to proportional mixing of temperature and salinity is used to quantify the density increase and mass convergence due to cabbeling.

4.1. Meridional Sections of Fractional Contributions

[19] Useful water mass analysis requires clear identification of source waters from which all other waters in the analysis are derived as a mixture. As described in section 2, average subtropical and subpolar waters are chosen as the sources, following *Talley et al.* [1995], *Talley* [1997] and *Talley and Yun* [2001]. These source waters are equivalent to the main two water masses in *Yasuda et al.*'s [1996] analysis of MWR. The subtropical source is chosen as the warmest and saltiest and the subpolar source as the coldest and freshest water in the region (Figure 2b). The subtropical source water (Figure 2b) was obtained by averaging temperature and salinity profiles from three Kofu-maru CTD stations south of the Kuroshio Extension: 41 (34.0°N, 144.0°E), 42 (34.3°N, 144.0°E) and 43 (34.66°N, 144.0°E). These three profiles were warm and saline and were located well away from the influence of Japan's coastal waters. The subpolar source water is an average of 6 Kofu-maru stations, 22 (42.3°N, 145.0°E), 23 (42.6°N, 144.9°E), 24 (43°N, 146°E), 53 (42°N, 144°E), and 54 (42.5°N, 144°E). These stations were located in the southward path of the Oyashio. The number of stations averaged in defining the subpolar source water mass was larger than for the subtropical water to remove local effects as much as possible and also because of shallow bottom depths at some stations. Experiments to test the sensitivity of the analysis to different selections of profiles for the source water masses showed that the solutions are substantially stable for reasonable choices.

[20] Figure 3a shows the relative contribution of the subtropical and the subpolar waters at 144°E based on the least squares analysis outlined in section 2. The main features are similar to those shown by *Talley and Yun* [2001] for a section at 152°E, based on simple proportional mixing between the source waters. Vertical sections of potential temperature, salinity and potential density at 144°E were presented by *Talley et al.* [1995]. The contour lines corresponding to 1 or 0 in Figure 3 are the regions where the temperature and salinity are higher than those of the subtropical water or lower than those of the subpolar water, respectively. Values greater than 0.9 are identified as subtropical water and those less than 0.1 as subpolar water. The values between 0.5 and 0.9 are defined as the "subtropical transition water" and those between 0.1 and 0.5 as the "subpolar transition water," approximately following *Talley et al.* [1995]. The region between 36°N and 40°N is occupied by the transition water [*Talley et al.*, 1995]. The two source water masses are apparent, with the warm subtropical water (warm core ring) to the south and the cold subpolar water to the north. At densities less than $26.7\sigma_\theta$ and greater than $27.3\sigma_\theta$ the influence of the subtropical water is stronger than the subpolar water up to 40°N, as also seen in the work of *Talley* [1997]. But at densities between $26.7\sigma_\theta$ and $27.3\sigma_\theta$ the subpolar water influence is substantial. (The depth of the isopycnal $26.7\sigma_\theta$ is 600 m in the warm core ring and 460 m in the region of the cold water intrusion.)

[21] The RMS best fit error for fractional contributions between 0.1 and 0.9 at 144°E (Figure 4) was on the order of 10^{-3} for densities lower than $27.0\sigma_\theta$, 10^{-4} for the density range $27.0-27.3\sigma_\theta$, and 10^{-5} for those higher than $27.3\sigma_\theta$, indicating a good fit. The RMS best fit errors were slightly higher in the density range $26.4-26.7\sigma_\theta$ with maxima at $26.4\sigma_\theta$ (1.6×10^{-3}), $26.54\sigma_\theta$, $26.61\sigma_\theta$, and $26.66\sigma_\theta$ (1.1×10^{-3} for the last three). White areas in Figure 4 indicate the regions where the observed temperature and salinity are higher than those of the subtropical source water or lower than those of the subpolar source water. Figure 4 shows that the RMS best fit error decreases monotonically with depth in the transition water region, away from subtropical or subpolar water, except in the density level less than $27.0\sigma_\theta$. This reflects the importance of cabbeling, discussed in section 5, for the misfit water mass fractions, and hence suggests that the measurement error contribution is small.

[22] The 152°E sections (Figure 3b) are located at the eastern edge of the MWR and were analyzed for fractional contributions of subtropical and subpolar waters by *Talley and Yun* [2001]. The waters of densities $26.5-27.5\sigma_\theta$ between the Kuroshio Extension and Subarctic Front are much better mixed than at 144°E; they are essentially the new NPIW [*Talley et al.*, 1995]. The waters on the 1981 and 1982 occupations are similar. The latitude coverage is better in the 1982 section, so we present it alone (Figure 3b). Subpolar water is found at 42°N with the water mass boundary at 41°N. The subtropical transition water covers most of the region shown: 28°N to 41°N. The fractional contribution of the subtropical water appears to be slightly larger ($\sim$0.9) at 26.4 to $26.5\sigma_\theta$, around 27.1 and 27.4 to $27.6\sigma_\theta$ with typical RMS best fit errors (figure not shown) of 4×10^{-4}, 5×10^{-5} and 2.5×10^{-6}, respectively. The maximum errors are very slightly larger than 0.001 and are found at $26.4\sigma_\theta$, $26.57\sigma_\theta$, $26.61\sigma_\theta$, and $26.66\sigma_\theta$. Compared with the 144°E section, the water mass south of 42°N is relatively more homogeneous subtropical transition water. This suggests that mixing occurs between the two sections and that there is less intrusion of the subpolar water at 152°E. The least squares procedure thus quantifies the water mass analysis of *Talley et al.* [1995] and the proportional mixing analysis of *Talley and Yun* [2001].

[23] The sections at 165°E lie well east of the MWR. Since the 1983 and 1984 sections have similar features

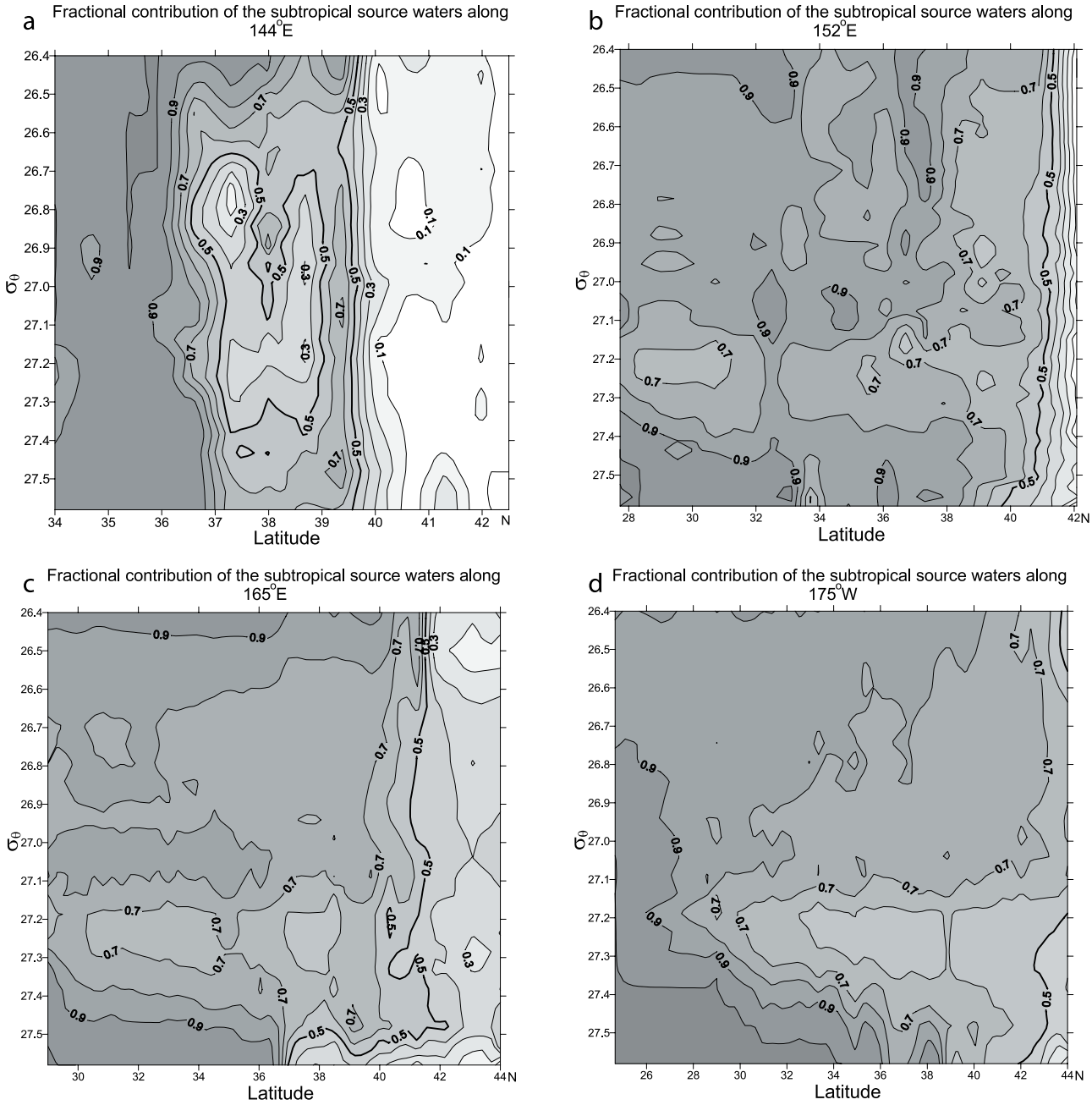

Figure 3. Fractional contribution of the subtropical source waters at (a) 144°E, (b) 152°E (1982), (c) 165°E (1984) and (d) 175°W.

except for the presence of a weak eddy in 1984 [*Joyce*, 1987], only the 1984 section is shown (Figure 3c). The boundary between the subtropical and the subpolar transition waters is at about 41°N. The subpolar water does not appear on this section up to the northernmost latitude sampled: 44°N. Subtropical water is present at 26.4, 27.1 and 27.4–27.6σ_θ but its contribution is smaller than at 152°E. The influence of the subpolar source water at around 27.2σ_θ appears to be slightly larger at 165°E than at 152°E. The homogeneity of the water mass is greater than at 152°E, presumably due to continued mixing as water moves from 152°E to 165°E. The RMS best fit errors (not shown) are more homogeneously distributed than at 144°E (Figure 4) and 152°E. The regions where the observed temperature and salinity are higher than those of the subtropical source water or lower than those of the subpolar source water are also much smaller than at 144°E (white areas in Figure 4). As for the other sections, slightly higher RMS best fit errors are found at 26.4–26.7σ_θ, compared with other densities, with the maxima at 26.4σ_θ (1.8×10^{-3}), 26.54σ_θ, 26.61σ_θ, and 26.66σ_θ (1.1×10^{-3} for the last three).

[24] The easternmost sections examined are at nearly the longitude of the Emperor Seamounts, at 175°W (Figure 3d). The water mass boundary appears to be north of 44°N. Subpolar transition water is seen only slightly at 44°N. Most of the section shows homogeneous coverage by the

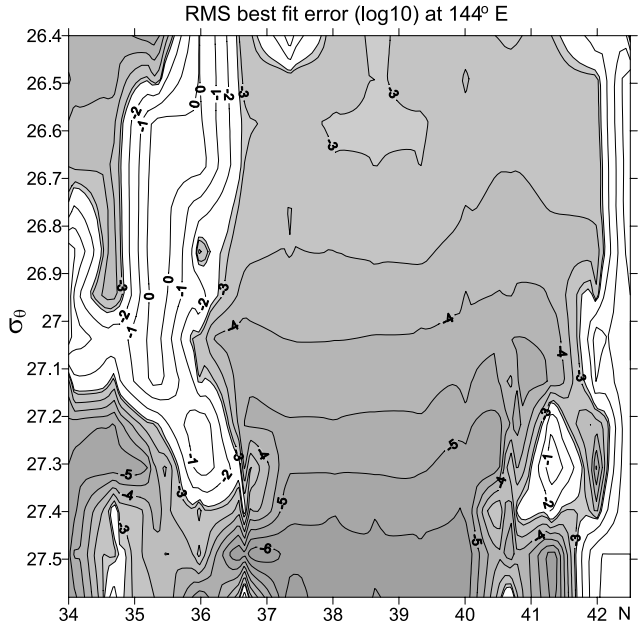

Figure 4. RMS best fit error (in log10) at 144°E. White areas are the regions where the observed temperature and salinity are higher than those of the subtropical source water or lower than those of the subpolar source water.

subtropical transition water except at 26.4, 26.8 to 27.3σ_θ south of 27°N, and 27.4 to 27.6σ_θ south of 36°N. In these regions the subtropical water is stronger. At densities higher than 27.1σ_θ there appears to be slightly more subpolar water influence, as in the more western sections. The RMS best fit errors (figure not shown) are distributed more homogeneously than on the other sections. Again as with the other sections, the errors are slightly larger at densities of 26.4 to 26.7σ_θ, with the maxima at 26.4σ_θ (1.8×10^{-3}), 26.54σ_θ, and 26.61σ_θ (1.2×10^{-3} for the last two).

[25] In summary, the boundary between the subtropical and the subpolar water masses shifts northward from 144°E to 175°W. That is, it is located at 40°N at 144°E, at 41°N at 152°E and 165°E and at 44°N at 175°W. As one proceeds from west to east, the water mass becomes more homogeneous, probably due to continuous mixing. The subtropical transition water becomes more dominant toward the east [*Talley et al.*, 1995]. The RMS best fit errors are largest at densities of 26.4–26.7σ_θ with a secondary group of error maxima at 26.61–26.66σ_θ.

4.2. Fractional Contributions of Source Waters on Isopycnals

[26] Using the data listed in Table 1 the fractional contributions of the subtropical and subpolar waters were calculated for each isopycnal. Since the stations were distributed irregularly over the region (33.8°N to 42.8°N, 140.5°E to 152.2°E), the contributions were objectively mapped to a regular grid. The x and y correlation length scales, the axis rotation angle and size of the error were tuned to obtain a realistic and smooth map. The choices were 45 km, 40 km, 60° and 0.15, respectively. The mapped data compared well with the 144°E and 152°E sections. Objective maps were produced at 0.01σ_θ intervals from 26.4 to 27.6σ_θ. Only three are shown here (Figure 5): at the top of the density range (26.4σ_θ), the bottom (27.5σ_θ), and at 26.8σ_θ, which is slightly denser than the local NPIW salinity

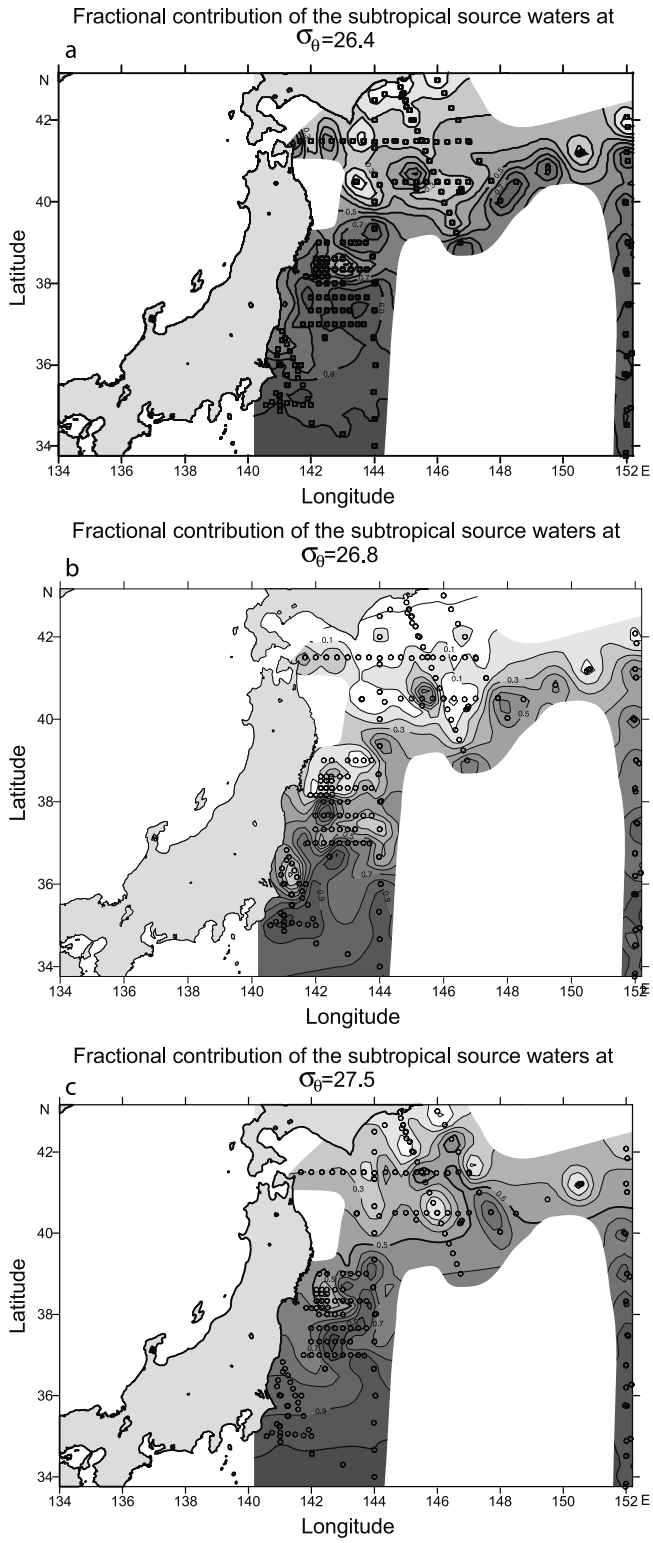

Figure 5. Fractional contribution of the subtropical source waters at (a) 26.4σ_θ, (b) 26.8σ_θ, and (c) 27.5σ_θ. Superimposed on this figure are the data points shown in Figure 2a.

minimum. Despite the nonsynopticity of the Japanese stations west of 144°E and the U.S. stations at 152°E sections, the latter are included to fill the eastern part of the region.

[27] The boundary between the subtropical and the subpolar waters, as indicated by the 0.5 contour, is located at 40°N to 41°N in Figures 5a and 5c. The 0.5 contour is found farthest south in the density range 26.7 to 26.9σ_θ, compared with other isopycnals, that is, at 37°N between 142°E and 144°E (Figure 5b). This southward excursion is a filament of Oyashio near-surface water that is wrapped around and down into the massive warm core ring at this location in this data set [*Talley et al.*, 1995; *Talley and Yun*, 2001]. From the vertical profiles shown in the previous papers, this is a primary mixing site between the Oyashio and Kuroshio waters and hence a primary location for cabbeling. In the coastal region the 0.5 contour is south of 36°N. This is also a southward intrusion of Oyashio water sandwiched between layers of Kuroshio water. Therefore, the area covered by the subpolar and its transition water is largest at this density. This interval of 26.7 to 26.8σ_θ is that of the NPIW.

[28] There are several locations where subtropical transition waters are found within the subpolar transition water region. For example, a warm eddy is present at 41°N, 146°E on all isopycnal surfaces (Figure 5). The Tsugaru water appears as a high subtropical fraction at 41.5°N, 142°E to 143°E. Its contribution is large in the range 26.4 to 26.6σ_θ but it is completely missing at 27.0σ_θ [*Hanawa and Mitsudera*, 1986; *Talley et al.*, 1995]. The most complex structure is found at 36.5°N to 40°N, 141°E to 144°E, in the center of the MWR [*Kawai*, 1972]. In this region all four water masses, that is, the subtropical, the subpolar and the transition waters of both, are present [*Talley et al.*, 1995; *Yasuda et al.*, 1996]. The Oyashio and Kuroshio separate from the western boundary to the north and south of this region. The separated currents generate meanders and eddies. The dynamically changing boundary between the water masses makes this an active mixing region. *Talley and Yun* [2001] showed that there was major vertical interleaving between nearly pure subpolar and subtropical intrusions in this region, and that the mixing zones lying vertically between the intrusions could be characterized by salt fingering or diffusive layering. (All mixing, regardless of its mechanism, is accompanied by cabbeling.)

5. NPIW Density, Cabbeling, and NPIW Mass Convergence

[29] The difference in temperature and salinity between the subtropical and subpolar waters is greatest at densities 26.4σ_θ and at 26.61–26.66σ_θ. The associated density increase due to cabbeling at 26.6σ_θ was shown previously by *Talley and Yun* [2001] to be about 0.07σ_θ (Figure 2). The density 26.6σ_θ is that of the Oyashio/Kamchatka Current winter surface water [*Reid*, 1973; *Talley*, 1991, 1993; *Talley et al.*, 1995], and the density that it cabbels to after mixing with the subtropical source water is nearly the NPIW salinity minimum density. (*Talley and Yun* [2001] also hypothesized that double diffusive processes in the intrusions in the western MWR lead to a density increase during mixing and estimated a effective flux ratio of 0.8 based on the observed density increase minus that which derives from cabbeling.)

[30] The water mass distributions in section 4.1 were calculated assuming that the two sources and their mixture are of the same density, that is, that $\rho = \rho_0$ in equation (2). However, the density of the mixture must be greater than that of the isopycnal sources due to cabbeling. Thus $x_1 + x_2$ in equation (2) is generally less than 1, and never greater than 1. We call

$$\gamma = 1 - x_1 - x_2 \tag{6}$$

the "misfit water mass fraction." The density increase due to cabbeling caused by the isopycnal mixing of two source waters and imposing mass conservation assuming $\rho_1 = \rho_2 = \rho$ in equations (1) and (2) together result in a non-zero misfit water mass fraction γ, as described in section 2. The large RMS best fit errors at densities lower than 27.0σ_θ (Figure 4) reflect a large misfit at these densities. The higher density water produced by cabbeling must sink (diapycnally). After noting the size and distribution of the misfits in the next few paragraphs, we then compute the density increase that reduces the misfit to zero for each observation. This approach, of iteratively finding the density increase that reduces the misfit to zero, is equivalent to finding the straight line in potential temperature/salinity space through each observation that connects source waters of the same density. We felt that using the misfits and iteration was a reasonable approach.

[31] Once the density increase that reduces the misfit to zero is obtained, the increase can be used to calculate diapycnal transport, which is the volume of water sinking per unit time from its original density level to the higher density, and which results from cabbeling. Transport convergence is then computed, showing a net convergence into the NPIW salinity minimum layer.

[32] The misfit water mass fraction γ at 144°E (Figure 6a) is large at the top (26.4σ_θ) and at 26.5 to 26.7σ_θ with a maximum around 26.6σ_θ. It is negligible below 27.0σ_θ. The large misfit at the upper level is due to especially large differences in temperatures and salinities between the two source water masses (Figure 2b), due to fresh coastal water, which lowers the subpolar near-surface salinity. The negligible misfit below 27.0σ_θ is due to the small temperature and salinity differences between the two source water masses. Zero misfit was assigned to some regions south of 36°N and north of 42°N in Figure 6a, where the observed temperature and salinity were higher than those of the subtropical source water or lower than those of the subpolar source. Thus the misfits here are actually very large (white area in Figure 4). We have neglected these computationally generated large misfits because cabbeling is negligible between two source waters of nearly the same temperature and salinity. In the subtropical and subpolar transition waters a large misfit occurs near 26.6σ_θ, which is the winter surface and mixed-layer density in the Oyashio/Kamchatka Current region.

[33] Farther to the east, at 152°E, 165°E (Figure 6b), and 175°W, the misfit water mass fractions are more homogeneous than at 144°E, probably due to continued mixing [*Talley et al.*, 1995], with an associated increase in density

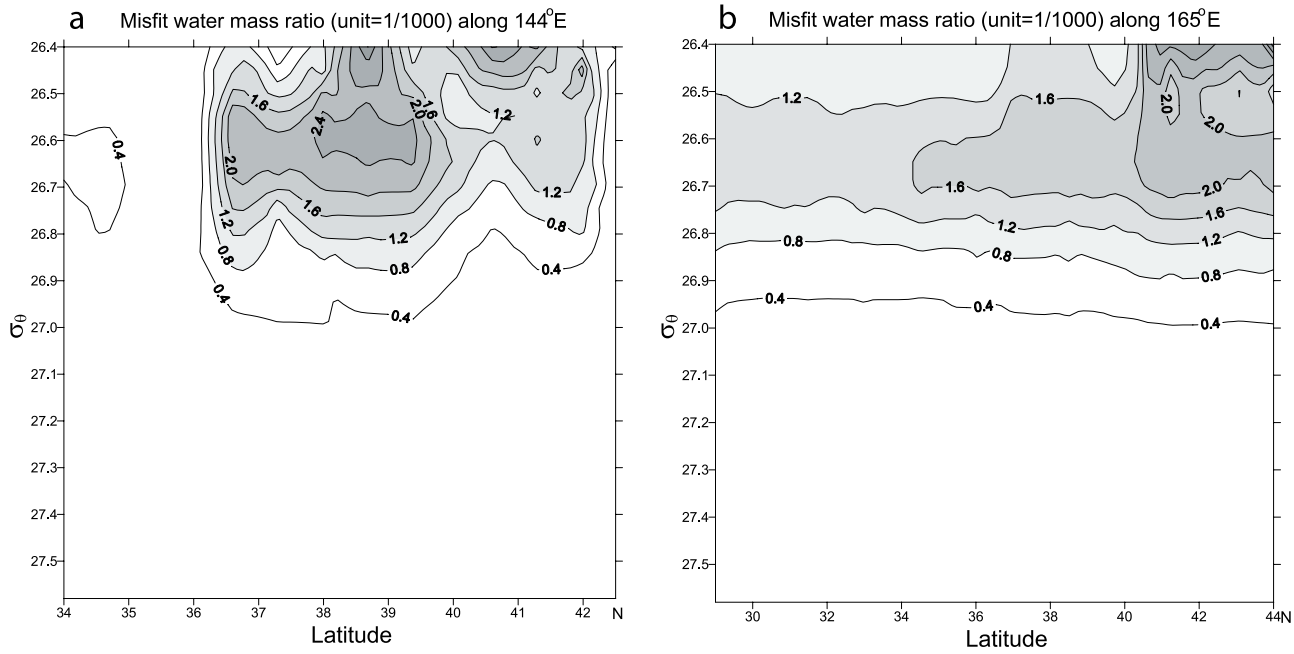

Figure 6. Misfit water mass fraction $\gamma = 1 - x_1 - x_2$ at (a) 144°E and (b) 165°E (1984). Labeled values are multiplied by 1000.

of the NPIW due to cabbeling. The misfits decrease more monotonically to the south as one moves from west to east. (We present only the 1984 165°E section in Figure 6b because the misfit and the corresponding density increases are similar on all of these eastern sections.)

[34] The maximum misfit occurs at the water mass boundary because cabbeling is largest when the fractional contributions x_1 and x_2 of subtropical and subpolar source waters are closest to each other, that is, when straight line mixing is farthest from the original isopycnal (Figure 2b). The maximum misfit in each section to the east occurs at a slightly higher density than at 144°E but it does not change much east of 152°E (see also Figures 7b–7d for the misfit ratio integrated over latitude band). The latitude of max-

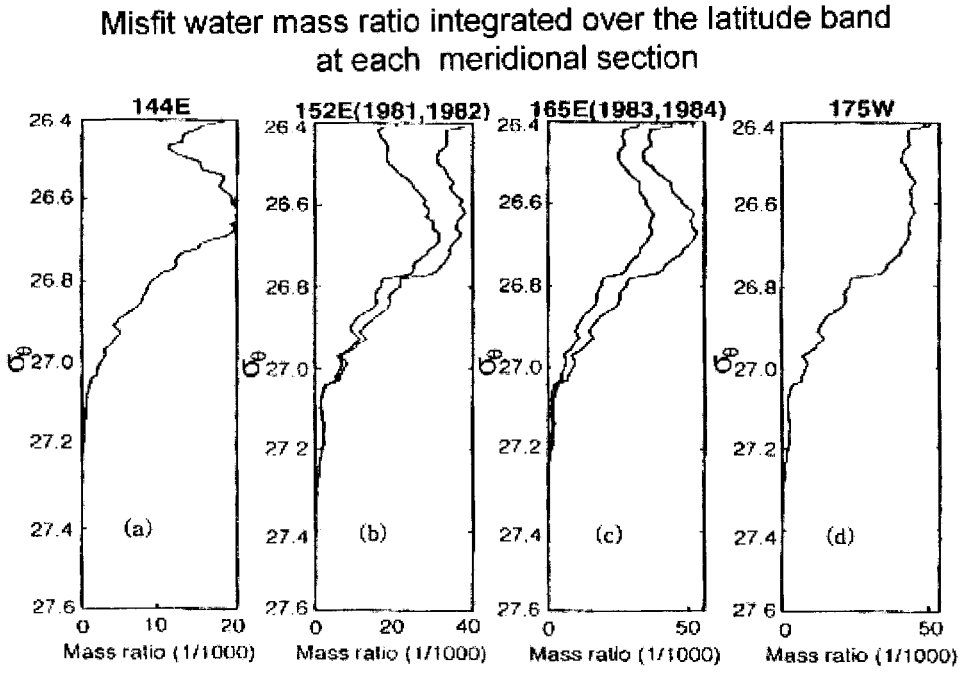

Figure 7. Misfit water mass fraction integrated over latitude for (a) 144°E, (b) 152°E (1981, 1982), (c) 165°E (1983, 1984) and (d) 175°W. Labeled values are multiplied by 1000.

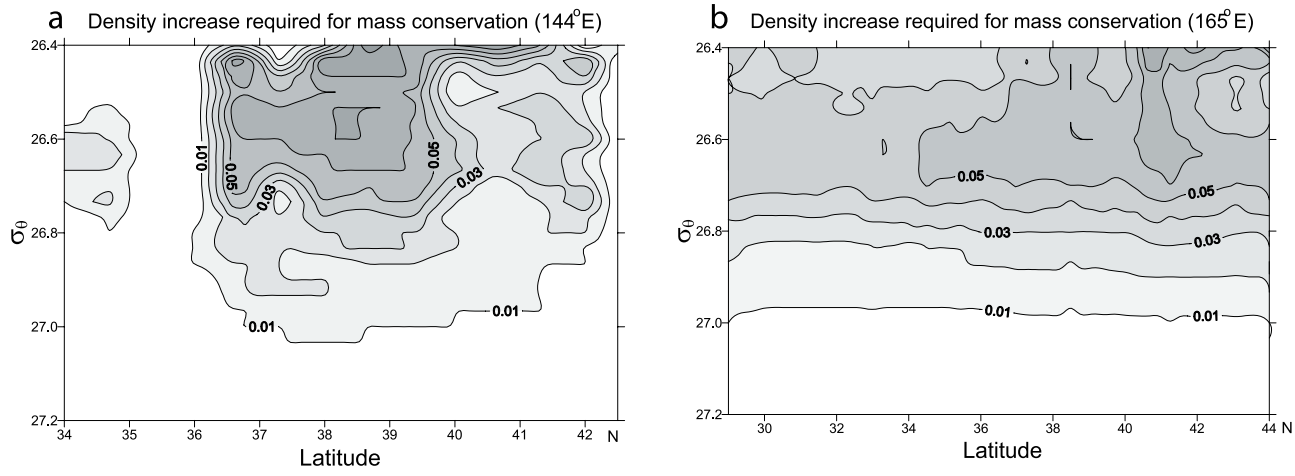

Figure 8. Density increase (in kg m^{-3}) required for heat, salt, and mass conservation at (a) 144°E and (b) 165°E (1984).

imum misfit shifts slightly northward from west to east, that is, from about 40°N at 152°E to about 42°N at 175°W. This tendency is also found in the water mass boundary between the two source waters, discussed in section 4.

[35] The misfit water mass fraction represents the lack of exact conservation of heat and salt due to cabbeling during mixing along isopycnals and is thus proportional to the density increase due to cabbeling. This density increase results in diapycnal transport. Diapycnal divergence of this sinking transport reduces the amount of water in isopycnal layers, and diapycnal convergence results in piling up of water, which then spreads out in isopycnal layers, before isopycnal circulations may bring layer thicknesses to steady state. The misfit fractions were integrated along isopycnals on each of the six meridional sections (Figure 7), yielding a quantity roughly proportional to net diapycnal transport. (Actual diapycnal transport is calculated below with a different method.) A positive gradient of the misfit, for example at the density range of 26.47–26.65σ_θ in Figure 7a, indicates net transport of water out of the density range. On the other hand, a negative gradient of the misfit, for example at the densities higher than 26.65σ_θ in Figure 7a, indicates net transport of water into these density levels with a larger gradient related to more volume transport. Thus the diapycnal gradients of the integrated misfits in Figure 7 are related to net mass convergence ($\partial\gamma/\partial\sigma_\theta < 0$) or divergence ($\partial\gamma/\partial\sigma_\theta > 0$). The maximum integrated misfit fractions at 144°E occur at 26.61 to 26.66σ_θ (Figure 7a) with a sign change in the diapycnal gradient at 26.68 to 26.70σ_θ, indicating a net flux of mass into this layer, which corresponds to the NPIW salinity minimum. At 165°E the maximum integrated misfit fractions occur at 26.67σ_θ (Figure 7c) with a sign change in the diapycnal gradient at 26.70σ_θ, also indicating a net flux into the NPIW layer.

[36] The effect of cabbeling can be quantified by re-examining equations (1) and (2) and calculating the density increase required to conserve mass, temperature and salinity. Since the existence of the misfit water mass fraction (equation (6)) indicates that the three equations in (1) and (2) do not hold exactly at that density level, we find the density level that satisfies the three conservation equations by moving down through the potential temperature and salinity of each profile in increments of 0.01σ_θ until the misfit is minimized (Figure 1). (This is equivalent to determining the density of the subtropical and subpolar source waters that would produce a given observed potential temperature/salinity through mixing along a straight line in the potential temperature/salinity plane.) The results are shown in Figure 8, which suggests how many density levels (with 0.01σ_θ interval) the completely mixed water of the subtropical and subpolar source waters would sink through due to cabbeling at 144°E and 165°E. At 144°E (Figure 8a) the maximum density increase, of 0.09σ_θ, occurs at the top level and is 0.07σ_θ at about 26.6σ_θ in the latitude band 38°N to 39°N, as shown by *Talley and Yun* [2001]. Therefore, cabbeling is active around 26.6σ_θ and the density of completely mixed water at this density level will increase by as much as 0.07σ_θ, to 26.67σ_θ. This is a downward vertical transport of the volume of the mixed water from 26.60 to 26.67σ_θ. The values in Figure 8 are then used to calculate the net diapycnal transport convergence. A similar increase in density is required for mass conservation on the other sections to the east, as discussed for the misfit water mass fraction in Figure 6. At 165°E (Figure 8b), however, the maximum density increase is slightly smaller than at 144°E and it occurs at densities slightly greater than 26.6σ_θ. The maximum density increase is also found at a more northern latitude at 165°E than at 144°E.

[37] The sinking transport due to cabbeling can be calculated at each density level at each station. The diapycnal volume transport in terms of diapycnal velocity w_σ is

$$T_\sigma = \int\int w_\sigma dxdy = \int\int \frac{dz}{dt} dxdy = \int\int \frac{\partial\rho}{\partial t}\frac{\partial z}{\partial\rho} dxdy$$

$$\approx \int\int \frac{\Delta\sigma_{cabbel}}{\Delta t}\frac{\Delta z}{0.01\ kgm^{-3}} dxdy$$

$$\approx \frac{\Delta x}{\Delta t}\sum_{i,j}\frac{\Delta\sigma_{cabbel}}{0.01\ kgm^{-3}}\Delta y_i \Delta z_j, \qquad (7)$$

where $\Delta\sigma_{\mathrm{cabbel}}$ is the density increase due to cabbeling, Δy_i is the meridional distance assigned to each station, Δz_j is the separation between isopycnals taken to be $\sigma_\theta = 0.01$ apart,

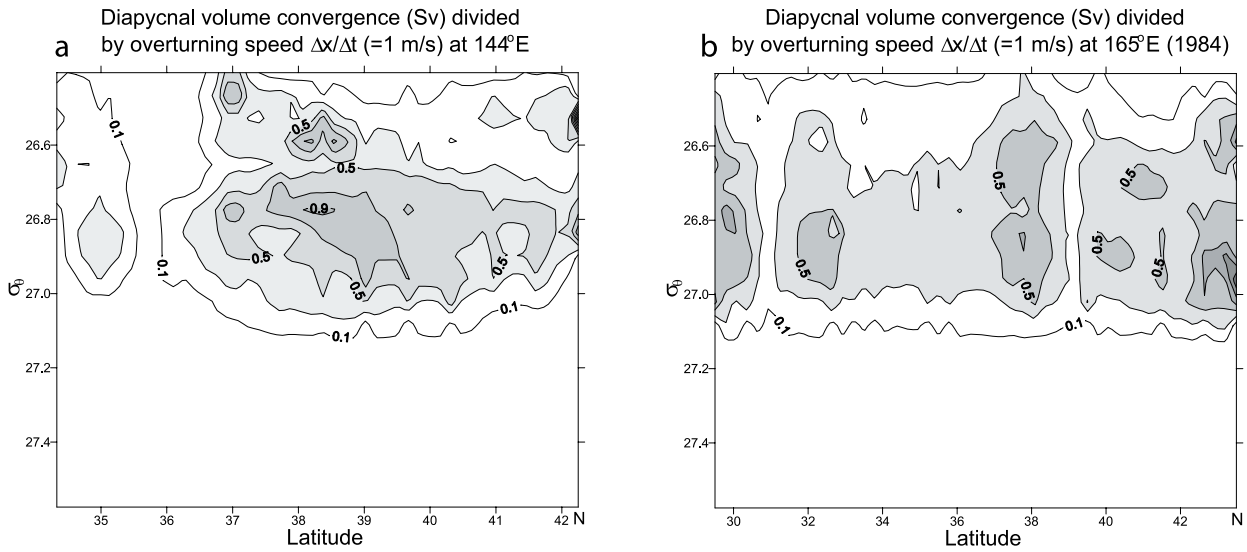

Figure 9. Diapycnal transport convergence (Sv) with $\Delta x/\Delta t = 1$ m/s at (a) 144°E and (b) 165°E (1984). The values are actually the diapycnal sinking area, $\Delta y_i \Delta z_j$, at each station and density surface.

and $\Delta x/\Delta t$ is the ratio of a longitudinal separation to the time estimated for complete mixing. This diapycnal volume transport moves a volume of water, $\Delta x \Delta y_i \Delta z_j$, in a time of Δt from a density level, σ_θ, before mixing due to cabbeling to a density level, $\sigma_\theta + \Delta\sigma_{\text{cabbel}}$, that satisfies the three conservation equations. The diapycnal transport convergence is the diapycnal volume transport into a density level minus the diapycnal volume transport out of the same density level. The quantities shown in Figures 9 and 10 are transport convergences in this sense.

[38] The diapycnal transport (equation (7)) is evaluated at the original density before the misfit is minimized. The values to be evaluated for each location are the isopycnal separation and $\Delta\sigma_{\text{cabbel}}$ (Figure 1). $\Delta\sigma_{\text{cabbel}}$ is calculated above by requiring mass, temperature, and salinity to be conserved exactly, through the procedure of minimizing the misfit γ, as described above. The distributions of $\Delta\sigma_{\text{cabbel}}$ for the 144°E and 165°E sections are shown in Figures 8a and 8b. Δz_j is the mean separation between the evaluated isopycnal and the isopycnals $\sigma_\theta = 0.01$ just above and just below. Δy_i is evaluated as the mean separation between the given station location and the two adjacent stations. Assigning a longitudinal width Δx is slightly more problematic because of the low longitudinal resolution, and is somewhat arbitrarily taken as the distance from the section in question to the next section to the east. The timescale Δt is the most difficult part to assign; our choices are discussed below.

[39] Since our data are along meridional sections, we first present just the portion $\Delta y_i \Delta z_j (\Delta\sigma_{\text{cabbel}}/0.01 \text{ kg m}^{-3})$ of the diapycnal transport, with units of area. Results at 144°E and 165°E are shown in Figure 9. The largest convergence in sinking "transport," $\Delta y_i \Delta z_j$, occurs at about $26.8\sigma_\theta$ (Figure 9a); the latter is the NPIW density. The large transport convergence at densities less than $26.6\sigma_\theta$ is because of unusually large thickness Δz_j in this data set due to an encounter of cold and fresh water with warm and saline water of a strong anticyclonic eddy [*Talley et al.*, 1995; *Talley and Yun*, 2001]. The maximum diapycnal transport convergence at 165°E in 1984 (Figure 9b) is also at about $26.8\sigma_\theta$, which is the NPIW density. Large transport convergence below $26.8\sigma_\theta$ is also found due to continuous mixing within the NPIW layer.

[40] The total diapycnal transport convergence for each section at each density is obtained by integrating $\sum_i \Delta y_i \Delta z_j$ over latitude. The results are shown in Figure 10, still in units of area since zonal length and time have not yet been assigned. Convergence of sinking transport into the NPIW layer is indicated by the occurrence of the higher peak at

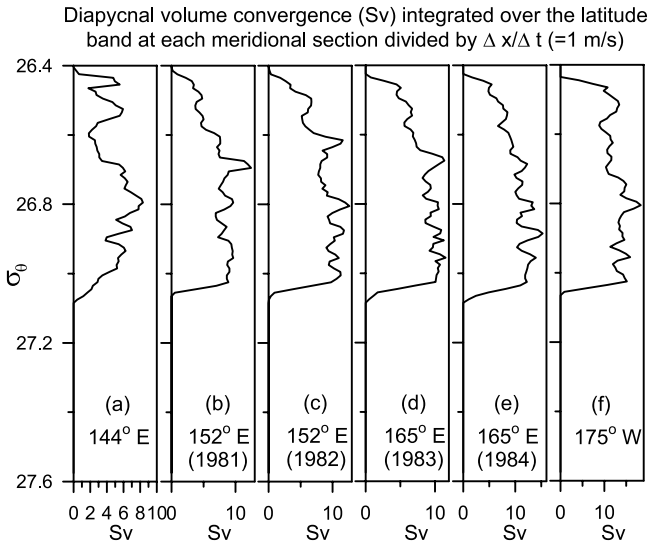

Figure 10. Diapycnal transport convergence (Sv) integrated over latitude, with $\Delta x/\Delta t = 1$m/s, at (a) 144°E, (b) 152°E (1981), (c) 152°E (1982), (d) 165°E (1983), (e) 165°E (1984), and (f) 175°W. The values are actually the diapycnal sinking area of Figure 9 integrated over latitude, $\sum_i \Delta y_i \Delta z_j$.

Table 2. Calculation of Diapycnal Transport Convergence in Each Subregion[a]

Subregion	Longitude Interval	Section	Sinking Area, 10^6 m^2 $\left(\sum_{i,j} > \Delta y_i \Delta z_j\right)$	Longitudinal Distance, 10^5 m (Δx)	Diapycnal Convergence, Sv $\left(\frac{\Delta x}{\Delta t}\sum_{i,j}\Delta y_i \Delta z_j\right)$
I	142°E–152°E	144°E	20.14	8.70	$0.56/\Delta t_1$
II	152°E–165°E	152°E (1982)	36.11	11.81	$1.35/\Delta t_2$
III	165°E–175°W	165°E (1984)	52.33	17.78	$2.95/\Delta t_3$
IV	175°W–136°W	175°W	53.62	35.03	$5.98/\Delta t_4$

[a]The diapycnal transport convergence listed here is the net transport of a volume of water produced by cabbeling into the NPIW layer. The density ranges of NPIW summation are 26.70–27.07σ_θ at 144°E, 152°E and 165°E and 26.70–27.05σ_θ at 175°W. Here t_1, t_2, t_3, and t_4, are in units of years.

about 26.8σ_θ at 144°E (Figure 10a). In the sections east of 144°E the convergence is distributed over broader ranges of densities and generally higher peaks appear to occur at slightly higher densities than at 26.8σ_θ.

[41] The basin-wide diapycnal transport due to cabbeling in equation (7) and the associated transport convergence requires assignment of a zonal distance, Δx, to each section, for example, at 144°E, 152°E (1981), 165°E (1984) and 175°W (Figures 10a, 10b, 10e and 10f, respectively), and a turnover time, Δt. The transports in equation (7) can also be summed for a given complete layer, for instance, of the NPIW. Δx is chosen to be the average longitudinal distance between the meridional section used in the cabbeling estimate and the next section to the east. For example, to compute the diapycnal transport convergence into the NPIW in the region between 142°E and 152°E, the net convergences of the meridionally-integrated diapycnal transport (equation (7)) with Δx = 1 m and Δt = 1 s, which is same as the sinking area $\sum_i \Delta y_i \Delta z_j$ at 144°E in Figure 10a, are summed over the density range between 26.7σ_θ and the deepest density limit of significant cabbeling (27.07σ_θ), multiplied by Δx (average distance of 10° longitude for this section), and divided by Δt, the assumed turnover time. The transport convergences between 152°E and 165°E and between 165°E and 175°W are computed similarly. To compute the transport convergence east of 175°W, Δx is taken to be 39° of longitude, assuming the eastern boundary of the NPIW region to be at 136°W [*Talley*, 1993]. Considering the deepest density limit of significant cabbeling at σ_θ = 27.05–27.07 in each of the four meridional sections, the diapycnal transport convergence into the NPIW in each subregion can be estimated using the formula given in the right-hand column of Table 2.

[42] To obtain a reasonable estimate of the diapycnal transport convergence due to cabbeling in the region between two neighboring sections, we need to make a reasonable guess for the turnover time, the time that is needed to mix two source waters completely until no more cabbeling occurs. It is, however, difficult to estimate a reasonable turnover time applicable to the entire NPIW region. It is known that most fresh water input from the subarctic region and most vigorous mixing occur in the MWR region west of 152°E. Therefore, the turnover time would be shorter in the MWR than in the region to the east. In subregion I (142°E–152°E), we assume Δt_1 = 1 year as a typical turnover time, considering that the lifetime of eddies is from two months to a couple of years, and occasionally to several years in the Kuroshio and Oyashio regions [*Richardson*, 1983]. Then the diapycnal transport convergence in this region is 0.56 Sv. However, this may be an overestimate because complete mixing between the two source waters may not occur within 1 year. Consequently, in the region between 142°E and 152°E, the diapycnal transport convergence due to cabbeling may be a fraction of 0.56 Sv.

[43] In other subregions east of 152°E, it is much more difficult to guess the turnover time because of additional input of fresh water from the subarctic and also because of continuous mixing as both source waters move eastward. Since the mixing time between two source waters is likely closely related to their flow speeds, we make a rough guess for the turnover time in each subregion, considering the observed flow speeds at each section. The maximum eastward speeds at a depth of about 500 m are 40, 20, and 5 cms^{-1} at 152°E, 165°E, and 175°W, respectively [*Schmitz et al.*, 1987; *Joyce and Schmitz*, 1988]. Subsequently, the turnover times in subregions III (165°E–175°W) and IV (175°W–136°W) are assumed to be twice and 8 times as long as in subregion II (152°E–165°E). If we assume a turnover time of 1 year in subregion I, as discussed above, and 2 years in subregion II which is located well east of the MWR, we can then use Δt_1 = 1, Δt_2 = 2, Δt_3 = 4, and Δt_4 = 16 years (Table 2) and add the results from the four subregions to obtain a total NPIW diapycnal transport convergence of 2.3 Sv which is due to cabbeling. This value is close to the net transport (2.46 Sv) of subpolar water into the MWR in the density range of 26.64–27.0σ_θ as calculated by *Talley* [1997], and is also similar to the 2.3 Sv of overturn into the North Pacific Intermediate Water calculated from net transports across 24°N based on *Reid*'s [1997] circulation [*Talley*, 2003].

6. Summary

[44] *Talley and Yun* [2001] hypothesized that cabbeling and double diffusion increase the density of the NPIW salinity minimum from the Oyashio winter surface density to 26.7–26.8σ_θ in the Mixed Water Region (MWR) just east of Japan. In order to quantify this density increase and convergence of mass into the NPIW salinity minimum layer, an inverse (least squares) method [*Mackas et al.*, 1987] was adopted to compute the relative proportions of subtropical and subpolar source waters in the NPIW mixture in the MWR, using an assumption of linear isopycnal mixing of source waters with continuous vertical variation, rather than point sources. The assumed source waters were the subtropical and subpolar waters from the Kuroshio and Oyashio [*Talley et al.*, 1995]. The method was applied only to densities greater than 26.4σ_θ in order to minimize complications due to air-sea interaction. The Tsugaru Water was also neglected as a source water mass, since its effect is limited to a local area

[*Talley*, 1993; *Talley et al.*, 1995]. The misfit in mass resulting from the assumption of linear isopycnal mixing was identified as being due to cabbeling.

[45] The densification effect was large at the surface and at 26.5 to 26.7σ_θ (maximum at around 26.6σ_θ) and negligible below 27.0σ_θ. The importance of cabbeling is of course directly proportional to the difference in source water temperatures and salinities. East of 152°E the maximum effect of cabbeling occurred at a slightly higher density level than at 144°E. The latitude of maximum cabbeling shifted northward from west to east, in the same pattern as the water mass boundary. The maximum density increase due to cabbeling was about 0.07σ_θ at around 26.6σ_θ thus shifting the fresh Oyashio winter surface water to the NPIW salinity minimum density. The downward diapycnal transport was formulated and the resulting transport convergence into the salinity minimum density layer was quantified. The procedures for estimation of transport convergence can be summarized as (1) estimate density increase due to cabbeling, (2) estimate sinking area $\Delta y_i \Delta z_j$ at each density level where cabbeling occurs, (3) estimate convergence in sinking transport at each density level (sinking into a level minus sinking out of the level), (4) estimate the net convergence of the meridionally-integrated sinking area $\sum_i \Delta y_i \Delta z_j$, (5) sum $\sum_i \Delta y_i \Delta z_j$ over the entire NPIW layer (i.e., compute $\sum_{ij} \Delta y_i \Delta z_j$) and estimate Δx and Δt, and (6) finally, compute $\frac{\Delta x}{\Delta t} \sum_{i,j} \Delta y_i \Delta z_j$. For the NPIW density range of 26.70–27.07σ_θ, the diapycnal transport convergence in the westernmost subregion (142°E–152°E) is estimated to be up to 0.56 Sv and the total diapycnal transport convergence in the entire NPIW region is estimated to be up to 2.3 Sv, assuming turnover times of 1, 2, 4, and 16 years in subregions I, II, III, and IV, respectively. These results are similar in order of magnitude to You's (submitted manuscript) dianeutral transport of about 0.9 Sv into the NPIW, evaluated using *McDougall and You*'s [1990] expression for dianeutral velocity due to cabbeling, which is an entirely different method from that used here and depends on assumed diapycnal and isopycnal diffusivities. You (submitted manuscript) evaluated the relative importance of cabbeling, thermobaricity and double diffusion and found that cabbeling dominates. *Talley and Yun* [2001] found a somewhat more ambiguous result, with double diffusion potentially contributing a similar order of magnitude to diapycnal transport as cabbeling.

[46] Since the convergence of the sinking volumes is not insubstantial and is the same order of magnitude as the 2 Sv of surface water to NPIW overturn in the North Pacific [*Talley*, 2003], we suggest that cabbeling is responsible for setting the final density of the NPIW salinity minimum (at least in part, with double diffusion possibly also contributing to densification [*Talley and Yun*, 2001]). We suggest that it is also responsible for converging mass into the NPIW salinity minimum layer, validating our hypothesis [*Talley et al.*, 1995] that the Oyashio winter mixed layer is the freshwater source of the NPIW salinity minimum.

[47] **Acknowledgments.** We owe a great debt to the scientists who collected the CTD data used herein: M. Fujimura, T. Kono, D. Inagake, M. Hirai, K. Okuda, P. Niiler and T. Joyce, and to Y. Nagata who made the data available to L.D.T. D. Rudnick provided guidance in the essentials of inverse methods. L.D.T. was supported by the National Science Foundation's Ocean Sciences Division, grant OCE92-03880. J.Y.Y. was supported for his sabbatical leave by the Korea Naval Academy.

References

Fofonoff, N. P., Some properties of sea water influencing the formation of Antarctic bottom water, *Deep Sea Res.*, *4*, 32–35, 1956.

Foster, T. D., An analysis of the cabbeling intensity in sea water, *J. Phys. Oceanogr.*, *2*, 294–301, 1972.

Hanawa, K., and H. Mitsudera, Variation of water system distribution in the Sanriku Coastal area, *J. Oceanogr. Soc. Jpn.*, *42*, 435–446, 1986.

Hasunuma, K., Formation of the intermediate salinity minimum in the northwestern Pacific Ocean, *Bull. Ocean Res. Inst. 9*, 47 pp., Univ. of Tokyo, Tokyo, 1978.

Joyce, T. M., A note on the lateral mixing of water masses, *J. Phys. Oceanogr.*, *7*, 626–629, 1977.

Joyce, T. M., Hydrographic sections across the Kuroshio Extension at 165°E and 175°W, *Deep Sea Res.*, *34*, 1331–1352, 1987.

Joyce, T. M., and W. J. Schmitz, Zonal velocity structure and transport in the Kuroshio Extension, *J. Phys. Oceanogr.*, *18*, 1484–1494, 1988.

Kawai, H., Hydrography of the Kuroshio Extension, in *Kuroshio: Physical Aspects of the Japan Current*, edited by H. Stommel and K. Yoshida, pp. 235–352, Univ. of Wash. Press, Seattle, Wash., 1972.

Levitus, S., Climatological atlas of the World Ocean, *NOAA Prof. Pap. 13*, U.S. Gov. Print. Off., Washington, D.C., 173 pp., 1982.

Maamaatuaiahutapu, K., V. C. Garcon, C. Provost, M. Boulahdid, and A. P. Osiroff, Brazil-Malvinas confluence: Water mass composition, *J. Geophys. Res.*, *97*, 9493–9505, 1992.

Mackas, D. L., K. L. Denman, and A. F. Bennet, Least squares multiple tracer analysis of water mass composition, *J. Geophys. Res.*, *92*, 2907–2918, 1987.

McDougall, T., The relative roles of diapycnal and isopycnal mixing on subsurface water mass conservation, *J. Phys. Oceanogr.*, *14*, 1577–1589, 1984.

McDougall, T., and Y. You, Implications of the nonlinear equation of state for upwelling in the ocean interior, *J. Geophys. Res.*, *95*, 13,263–13,276, 1990.

Menke, W., *Geophysical Data Analysis: Discrete Inverse Theory*, *Int. Geophys. Ser.*, vol. 45, 289 pp., Academic, San Diego, Calif., 1989.

Niiler, P. P., W. J. Schmitz, and D.-K. Lee, Geostrophic mass transport in high eddy energy regions of the Kuroshio and Gulf Stream, *J. Phys. Oceanogr.*, *15*, 825–843, 1985.

Reid, J. L., Jr., Intermediate waters of the Pacific Ocean, *Johns Hopkins Oceanogr. Stud.*, *2*, 85 pp., 1965.

Reid, J. L., Jr., Northwest Pacific Ocean waters in winter, *Johns Hopkins Oceanogr. Stud.*, *5*, 96 pp., 1973.

Reid, J. L., Jr., On the total geostrophic circulation of the Pacific Ocean: Flow patterns, tracers and transports, *Prog. Oceanogr.*, *39*, 263–352, 1997.

Richardson, P. L., Gulf Stream rings, in *Eddies in Marine Science*, edited by A. R. Robinson, pp. 19–45, Springer-Verlag, New York, 1983.

Schmitz, W. J., Jr., P. P. Niiler, and C. J. Koblinsky, Two-year moored instrument results along 152°E, *J. Geophys. Res.*, *92*, 10,826–10,834, 1987.

Stommel, H., *The Gulf Stream*, 202 pp., Univ. of Calif. Press, Berkeley, Calif., 1960.

Sverdrup, H., M. W. Johnson, and R. H. Fleming, *The Oceans, Their Physics, Chemistry, and General Biology*, 1087 pp., Prentice-Hall, Old Tappan, N. J., 1942.

Talley, L. D., Ventilation of the subtropical North Pacific: The shallow salinity minimum, *J. Phys. Oceanogr.*, *15*, 633–649, 1985.

Talley, L. D., Potential vorticity distribution in the North Pacific, *J. Phys. Oceanogr.*, *18*, 89–106, 1988.

Talley, L. D., An Okhotsk sea water anomaly: Implications for ventilation in the North Pacific, *Deep Sea Res.*, *38*, Suppl., S171–S190, 1991.

Talley, L. D., Distribution and formation of North Pacific Intermediate Water, *J. Phys. Oceanogr.*, *23*, 517–537, 1993.

Talley, L. D., North Pacific Intermediate Water transports in the mixed water region, *J. Phys. Oceanogr.*, *27*, 1795–1803, 1997.

Talley, L. D., Shallow, intermediate and deep overturning components of the global heat budget, *J. Phys. Oceanogr.*, *33*, 530–560, 2003.

Talley, L. D., and J.-Y. Yun, Cabbeling, double diffusion and density of North Pacific Intermediate Water, *J. Phys. Oceanogr.*, *31*, 1538–1549, 2001.

Talley, L. D., Y. Nagata, M. Fujimura, T. Kono, D. Inagake, M. Hirai, and K. Okuda, North Pacific Intermediate Water in the Kuroshio/Oyashio mixed water region in Spring 1989, *J. Phys. Oceanogr.*, *25*, 475–501, 1995.

Van Scoy, K., D. B. Olsen, and R. A. Fine, Ventilation of North Pacific Intermediate Water: The role of the Alaskan Gyre, *J. Geophys. Res.*, *96*, 16,801–16,810, 1991.

Witte, E., *Zur Theorie der Strom Kabbelungen*, pp. 484–487, Gaea, Cologne, Germany, 1902.

Yasuda, I., K. Okuda, and Y. Shimizu, Distribution and modification of North Pacific intermediate water in the Kuroshio-Oyashio interfrontal zone, *J. Phys. Oceanogr.*, *26*, 448–465, 1996.

You, Y., Implications of cabbeling on the formation and transformation mechanism of the North Pacific Intermediate Water, *J. Geophys. Res.*, doi:10.1029/2001JC001285, in press, 2003.

You, Y., N. Suginohara, M. Fukasawa, I. Yasuda, I. Kaneko, H. Yoritaka, and M. Kawamiya, Roles of the Okhotsk Sea and Gulf of Alaska in forming the North Pacific Intermediate Water, *J. Geophys. Res.*, *105*, 3253–3280, 2000.

Zhang, R.-C., and K. Hanawa, Features of the water-mass front in the northwestern North Pacific, *J. Geophys. Res.*, *98*, 967–973, 1993.

L. D. Talley, Scripps Institution of Oceanography, University of California, San Diego, La Jolla, CA 92093-0230, USA. (ltalley@ucsd.edu)

J.-Y. Yun, Research Institute of Oceanography, Seoul National University, San 56-1, Sillim-dong, Kwanak-gu, Seoul 151-742, South Korea. (jyyun@ocean.snu.ac.kr)